

Random replicators with asymmetric couplings

Tobias Galla^{†‡}

[†] The Abdus Salam International Centre for Theoretical Physics, Strada Costiera 11, 34014 Trieste, Italy

[‡] CNR-INFM, Trieste-SISSA Unit, V. Beirut 2-4, 34014 Trieste, Italy

Abstract. The dynamics of random replicators is studied using generating functional techniques. While replica analyses are limited to models with symmetric couplings, dynamical approaches as presented here allow specifically to address cases with asymmetric interactions. We first discuss in detail how dynamical theories can be formulated for general replicator models in terms of an effective single-species process, and how persistent order parameters of the ergodic stationary states can be extracted from this process. We then detail how different types of dynamical phase transitions can be identified and related to each other. As an application of the general theory we address replicator models with Gaussian couplings of arbitrary symmetry between pairs and triples of species, respectively. Numerical simulations verify our theory, and also indicate regimes in which only a finite number of species survives, even when the thermodynamic limit is considered.

PACS numbers: 87.23-n, 87.10+e, 75.10.Nr, 64.60.Ht

E-mail: galla@ictp.trieste.it

1. Introduction

There is only a limited number of methods with which disordered systems occurring in statistical mechanics can be addressed efficiently. The difficulties in handling such systems root in the fact that it is essentially impossible to deal analytically with specific instances of the quenched random couplings, which generate a complicated structure of frustrated interactions and competing forces. Two of the most prominent approaches therefore address the *typical* static and dynamical behaviour of disordered systems, respectively, that is the statistical properties of the system averaged over all possible realisations of the disorder. Static methods are here concerned with the computation of the disorder-averaged logarithm of the thermodynamic partition function. The disorder-average is here typically performed based on replica methods and the computations rely on the existence of an energy (or Lyapunov) function, which defines the Boltzmann measure of the system. Once this measure is computed, static observables can be obtained as suitable averages. Dynamical methods on the other hand address the temporal evolution of the system, again on disorder-average. Here a dynamic partition functional (or generating functional) is defined as an integral over all possible trajectories

of the systems subject to the equations of motion. Upon introducing suitable source and perturbation fields, dynamic observables can then again be obtained as derivatives of the disorder-averaged generating functional. In contrast to replica methods this second approach does not require any Lyapunov function governing the dynamics of the system, but can be applied starting from the microscopic equations of motion. Generating functionals are therefore a powerful tool to address non-equilibrium disordered systems lacking detailed balance.

Both dynamic and static methods cannot only be applied successfully to study the behaviour of spin glasses and magnetic systems, but also to systems of interacting agents motivated by game theory, economics or biology. The dynamics and collective phenomena of interacting agents are currently studied intensively in the physics community for example in the context of the so-called Minority Game [1, 2, 3]. Replica theory and generating functionals have proved to be extremely powerful here.

The aim of the present paper is to discuss dynamical methods in the context of so-called random replicator models (RRM). These describe the evolution of self-reproducing interacting species within a given framework of limited resources and have found wide applications in a variety of fields including game theory, socio-biology, pre-biotic evolution and optimization theory [4, 5, 6]. While the first replicator system with quenched random couplings was introduced by Diederich and Opper in [7, 8], most subsequent studies in the statistical physics community seem to be based on replica theory or on computer simulations [10, 11, 12, 13, 14, 15, 16, 17, 18]. Thus most of the existing analytic work on RRM is restricted to the case of symmetric couplings, in which a Lyapunov function can be found, so that replica theory is applicable. The only exceptions appear to be the early papers by Rieger [19] and Opper and Diederich [8, 9], where RRM were studied using generating functional techniques.

We here extend the work of [8, 9] (which is concerned with pairwise Gaussian interactions) and discuss how dynamic methods can be applied to more general replicator systems. Without specifying the particular type of RRM (i.e. without fixing the statistics of the random couplings) will first show how a dynamical theory can be formulated in terms of a single effective-species process, and how persistent order parameters characterizing the ergodic stationary states can be extracted from this process. This procedure can be carried out irrespective of the symmetry of the couplings. We will then discuss different types of possible phase transitions and their relation to each other. Finally we apply our theory to the case of RRM with Gaussian couplings of general symmetry between pairs and triples of species, respectively, in direct extension also of [10], where the case of higher-order symmetric couplings with Gaussian distribution was addressed using replica theory.

2. General theory

2.1. Model definitions

Random replicator models describe systems of N interacting species labelled by Roman indices $i = 1, \dots, N$ with time-dependent concentrations $x_i(t) \geq 0$. The interactions governing the temporal evolution of the $\{x_i(t)\}$ are here assumed to be of the general form

$$\frac{d}{dt}x_i(t) = x_i(t) \left[f_i(\mathbf{x}(t)|\mathbf{J}) - \frac{1}{N} \sum_{j=1}^N x_j(t) f_j(\mathbf{x}(t)|\mathbf{J}) \right]. \quad (1)$$

Here $f_i(\mathbf{x}(t)|\mathbf{J})$ denotes the ‘fitness’ of species i at time t , and may depend on the full concentration vector $\mathbf{x}(t) = (x_1(t), \dots, x_N(t))$ at time t as well as on a set of random couplings \mathbf{J} . We will not specify the structure of the inter-species couplings and the statistics from which they are drawn at this stage, but will address specific cases later. We will choose initial conditions at time $t = 0$ such that

$$\frac{1}{N} \sum_i x_i(t=0) = 1. \quad (2)$$

Note that the set of differential equations (1) then conserves the total concentration $\sum_i x_i(t)$. In the following we will write

$$\frac{d}{dt}x_i(t) = -x_i(t) [-f_i(\mathbf{x}(t)|\mathbf{J}) - \kappa(t) + \sigma\zeta_i(t)], \quad (3)$$

where $\kappa(t)$ is chosen such that the constraint (2) is fulfilled at any time, and where we have added Gaussian white noise $\zeta_i(t)$ to the dynamics (with $\langle \zeta_i(t)\zeta_j(t') \rangle = \delta_{ij}\delta(t-t')$). The model parameter σ denotes the amplitude of this noise component.

2.2. Generating functional and effective process

Eqs. (3) define a set of N evolution equations, which are coupled to each other through the random interactions \mathbf{J} , and through the overall constraint (2). Note that a Lyapunov function which is extremised by this dynamics can be found only in the case of symmetric couplings. Replica methods may then be applied to identify the extrema of this random function, corresponding to the stationary states asymptotically reached by the system. In the general case one has to deal directly with the dynamics, and generating functionals originally developed by De Dominicis in the context of disordered systems [20] provide a powerful tool for the further analysis.

As a first step one adds perturbation fields $\{h_i(t)\}$ to the dynamics and starts from

$$\frac{d}{dt}x_i(t) = -x_i(t) [-f_i(\mathbf{x}(t)|\mathbf{J}) - \kappa(t) + \sigma\zeta_i(t) - h_i(t)], \quad (4)$$

the $\{h_i(t)\}$ are introduced to generate response functions at later stages, and will be set to zero at the end of the calculation. We will in the following assume that the fitness functions $f_i(\mathbf{x}|\mathbf{J})$ can be written in the form

$$f_i(\mathbf{x}(t)|\mathbf{J}) = f(x_i(t)) + g_i(\{x_j(t) : j \neq i\}|\mathbf{J}), \quad (5)$$

i.e. that f_i can be separated into a non-disordered contribution $f(x_i(t))$, depending only on the species concentration $x_i(t)$, and into an ‘off-diagonal’ term $g_i(\{x_j(t) : j \neq i\}|\mathbf{J})$ containing the disorder and depending on the concentrations $\{x_j(t)\}$ with $j \neq i$. The strength of the former contribution may depend on a uniform model parameter describing the strength of the self-interaction (the so-called ‘co-operation pressure’ [5]). This control parameter will generally be labelled by u in later sections. Extensions to non-uniform values of u are straightforward, but complicate the detailed mathematics of the further analysis.

The moment generating functional is then defined as

$$\begin{aligned} Z[\psi] &= \left\langle \left\langle \exp \left(i \sum_i \int dt \psi_i(t) x_i(t) \right) \right\rangle \right\rangle \\ &= \int D\mathbf{x} p_0(\mathbf{x}(0)) \exp \left(i \sum_i \int dt \psi_i(t) x_i(t) \right) \prod_{i,t} \delta[\text{Equation (4)}]. \end{aligned} \quad (6)$$

$\langle \langle \dots \rangle \rangle$ denotes an average over all possible paths of the system. $p_0(\mathbf{x}(0))$ describes the (possibly random) initial conditions from which the dynamics is started. All initial concentrations are taken to be strictly positive with probability one here.

The general procedure then consists in a computation of the disorder-averaged generating functional $\overline{Z[\psi]}$, from which dynamical order parameters can be computed as derivatives with respect to the fields $\{\psi_i(t), h_i(t)\}$. The aim is then to formulate a closed set of equations describing the temporal evolution of a set of suitable dynamical observables, which adequately describe the macroscopic dynamics. If we limit ourselves to extensively connected mean-field systems, the relevant order parameters for RRM are given by the Lagrange parameter $\kappa = \{\overline{\langle \kappa(t) \rangle}\}$ and the correlation and response functions $\{\mathbf{C}, \mathbf{G}\}$:

$$C(t, t') = \lim_{N \rightarrow \infty} \frac{1}{N} \sum_{i=1}^N \overline{\langle x_i(t) x_i(t') \rangle}, \quad G(t, t') = \lim_{N \rightarrow \infty} \frac{1}{N} \sum_{i=1}^N \frac{\delta \overline{\langle x_i(t) \rangle}}{\delta h_i(t')}. \quad (7)$$

Here $\langle \dots \rangle$ stands for an average over the white noise $\{\zeta_i(t)\}$ and over realisations of the initial conditions. Note that $G(t, t') = 0$ for $t \leq t'$ due to causality.

The computation of $\overline{Z[\psi]}$ is in general lengthy, but straightforward for common choices of the statistics of the set of couplings \mathbf{J} once a transformation $y_i(t) = \log x_i(t)$ has been performed. The necessary mathematical steps depend on the specific details of the distribution from which the \mathbf{J} are drawn. The final outcome of the theory in the limit $N \rightarrow \infty$ consists in a so-called ‘single effective-species process’ of the form

$$\frac{d}{dt} x(t) = -x(t) \left[f(x(t)) - \int_0^t dt' R(t, t') x(t') + \eta(t) + \sigma \zeta(t) - \kappa(t) - h(t) \right]. \quad (8)$$

We have here assumed that the perturbation fields are of the form $h_i(t) = h(t)$ for all i , and that the distribution of initial conditions factorizes over individual species $p_0(\mathbf{x}(0)) = \prod_i p_0(x_i(0))$. $\zeta(t)$ in (8) is white noise $\langle \zeta(t) \zeta(t') \rangle = \delta(t - t')$ and reflects the white noise in the initial N -species problem. $f(x(t))$ is the disorder-free self-interaction part, see Eq. (5).

The disorder in the dynamics of the original N species $\{x_i(t)\}$ has been traded for two ingredients of the effective process: firstly, we note the presence of a retarded self-interaction term $\int_0^t dt' R(t, t') x(t')$ and secondly that of an additional noise contribution $\eta(t)$, which in general will turn out to have non-trivial temporal correlations. The precise functional form of the self-interaction kernel $R(t, t')$ and of the covariance

$$\Lambda(t, t') \equiv \langle \eta(t) \eta(t') \rangle_* \quad (9)$$

depends on the type of interaction $g_i(\cdot | \mathbf{J})$ in the initial dynamics and on the type and statistics of the couplings \mathbf{J} . For mean-field interactions \mathbf{R} and $\mathbf{\Lambda}$ can generally be expressed in terms of the two-time correlation and response functions \mathbf{C} and \mathbf{G} .

These correlation and response functions \mathbf{C} and \mathbf{G} of the original multi-species system can in turn be shown to be given by

$$C(t, t') = \langle x(t) x(t') \rangle_*, \quad G(t, t') = \frac{\delta}{\delta h(t')} \langle x(t) \rangle_*, \quad (10)$$

and κ has to be chosen such that

$$\langle x(t) \rangle_* = 1 \quad \forall t. \quad (11)$$

Here $\langle \dots \rangle_*$ denotes an average over realisations of the effective process (8), i.e. over realisations of the single-species coloured noise $\{\eta(t)\}$, of the white noise $\{\zeta(t)\}$ and over initial conditions described by $p_0(x(0))$. Eqs. (8,9,10,11) thus form a closed set of equations from which $\{\kappa, \mathbf{C}, \mathbf{G}\}$ are to be obtained. These equations are exact and fully equivalent to the original N -species problem Eq. (3) in the limit $N \rightarrow \infty$. The retarded self-interaction and the coloured noise are direct consequences of the quenched disorder in the original problem and impede an explicit analytical solution of the self-consistent saddle-point problem. In similar disordered systems (such as the Minority Game) one is therefore usually limited to specific ansätze for the trajectories of the effective particles. Alternatively, effective dynamical problems in discrete time may be addressed using a Monte-Carlo integration of the single-particle process [24]. While this method allows to compute the dynamical order parameters numerically without finite-size effects the iteration quickly becomes costly in terms of computer time as the number of time-steps is increased. For similar disordered systems one is usually limited to $\mathcal{O}(100)$ iterations, the equilibration times for (suitably discretised) RRM however typically turn out to be much larger.

2.3. Stationary state

In order to proceed we assume that a stationary time-translation invariant (TTI) state is reached in the long-term limit, i.e. we will be looking for solutions of the following type

$$\lim_{t \rightarrow \infty} C(t + \tau, t) = C(\tau), \quad \lim_{t \rightarrow \infty} G(t + \tau, t) = G(\tau), \quad \lim_{t \rightarrow \infty} \kappa(t) = \kappa. \quad (12)$$

Within this ansatz the covariance matrix of the single-species noise and the kernel of retarded self-interaction also become TTI, $\Lambda(t, t') = \Lambda(t - t')$ and

$R(t, t') = R(t - t')$. It will then turn out to be convenient to introduce Fourier transforms $\{\tilde{C}(\omega), \tilde{G}(\omega), \tilde{\Lambda}(\omega), \tilde{R}(\omega)\}$ of the one-time functions $\{C(\tau), G(\tau), \Lambda(\tau), R(\tau)\}$ respectively. Furthermore we will only address ergodic stationary states, that is states in which perturbations have no long-term effects so that the integrated response function remains finite

$$\chi \equiv \tilde{G}(\omega = 0) = \int_0^\infty d\tau G(\tau) < \infty, \quad (13)$$

and no long-term memory is present, i.e. we will assume

$$\lim_{t \rightarrow \infty} G(t, t') = 0 \quad (14)$$

also for finite t' . In the absence of memory we may send the starting point of the dynamics to $-\infty$ for convenience. As in other disordered systems a specific ansatz needs to be made to address the stationary states reached by the effective process. We will henceforth restrict the analysis to the case $\sigma = 0$, in which the original problem (3) becomes fully deterministic once the disordered interactions and random initial conditions have been drawn. We will also assume that the system reaches a microscopic fixed point asymptotically, i.e. that the limits $x_i \equiv \lim_{t \rightarrow \infty} x_i(t)$ exist for all i . Although this may seem to be a considerable constraint, such fixed points are typically observed in simulations of many variants of the original random replicator model, as long as the self-interaction term in (5) carries sufficient weight to suppress runaway solutions and/or volatile trajectories (i.e. for large u). In particular even the trajectories of RRM with asymmetric couplings evolve into fixed points at large enough co-operation pressure so that restriction to this type of solution appears appropriate here as it simplifies the analysis considerably. Given this assumption we may look for solutions $x(t) \rightarrow x$ (with x a static random variable) of the effective process, resulting in a flat correlation function

$$q \equiv C(\tau) \quad \forall \tau \quad (15)$$

in the stationary state. Accordingly we also assume the single-species noise $\{\eta(t)\}$ approaches a fixed value η , which in turn is then a static Gaussian variable with zero mean and variance

$$\langle \eta^2 \rangle_* = \lambda, \quad (16)$$

where λ is defined by $\tilde{\Lambda}(\omega) = \lambda \delta(\omega)$. We also have $\int_{-\infty}^t dt' R(t, t') x(t') = \rho x$ in the stationary state, where ρ is the zero-frequency component of the retarded interaction kernel $R(t - t')$. Insertion of this fixed point ansatz into the effective process (8) leads to ($\sigma = 0$):

$$x \left[f(x) - \rho x + \sqrt{\lambda} z - \kappa \right] = 0, \quad (17)$$

where we have written $\eta = \sqrt{\lambda} z$ with a standard Gaussian variable z . $h(t)$ has been set to zero, note that (up to a pre-factor) the persistent response may equally be computed by taking derivatives of x with respect to z . For any given realization of the single-particle noise $\eta(t)$ and hence for every resulting value of the random variable z the corresponding fixed point $x(z)$ has to be determined from this equation. We first note

that $x(z) = 0$ is always a solution, irrespective of z . However positive fixed point values $x(z)$ may be possible if

$$f(x) - \rho x + \sqrt{\lambda}z - \kappa = 0 \quad (18)$$

has one or more positive roots. In general this will impose a constraint on z , i.e. positive solutions may exist only for values of z within a subset of the real axis. The measure of this subset will determine the probability for a species to survive in the long-run (i.e. to attain a fixed point $x(z) > 0$). For the moment we will ignore the potential multiplicity of the solutions of (17) and will assume that for any value of z a unique meaningful zero $x(z) \geq 0$ of (17) can be identified on physical grounds. We will also postpone a discussion of possible issues regarding the stability of the fixed points. We note that (18) implies

$$\frac{1}{\sqrt{\lambda}} \frac{\partial x}{\partial z} = -\frac{1}{f'(x) - \rho}. \quad (19)$$

(with $f' = df/dx$). Self-consistency then demands that the following relations hold:

$$1 = \int Dz \Theta[x(z)] x(z), \quad (20)$$

$$q = \int Dz \Theta[x(z)] [x(z)]^2, \quad (21)$$

$$\chi = \int Dz \Theta[x(z)] [f'(x(z)) - \rho]^{-1}. \quad (22)$$

Here $Dz = e^{-z^2/2} dz / \sqrt{2\pi}$ is a standard Gaussian measure, and $\Theta(y) = 1$ for $y > 0$ and $\Theta(y) = 0$ otherwise is the step-function. Only surviving species $x(z) > 0$ contribute to these order parameters. Under the assumption that ρ and λ may be written as functions of κ , of the asymptotic value q of the correlation function and of the integrated response χ relations (20)-(22) together with the prescription $x = x(z)$ form a closed set of equations for the order parameters $\{q, \chi, \kappa\}$ characterizing the ergodic stationary state.

We now turn briefly to an interpretation of the order parameter q , which within the fixed point ansatz is given by $q = \lim_{N \rightarrow \infty} N^{-1} \sum_i \overline{\langle x_i^2 \rangle}$. If the x_i were normalised to 1 instead of N , q would be closely related to what is known as Simpson's index of diversity [21] and would indicate the probability that two randomly selected individuals of the eco-system are of the same species. A Simpson index of zero thus indicates infinite diversity, a value of one corresponds to no diversity. A similar interpretation holds for the normalisation of the $\{x_i\}$ used here: finite values of q indicate the co-existence of an extensive number of species with concentrations $x_i \sim \mathcal{O}(N^0)$, while a divergence in q signals the dominance of a sub-extensive number of species with diverging concentrations in the thermodynamic limit [11]. We thus expect the behaviour of $1/q$ to be similar to that of the fraction of surviving species $\phi \equiv \int Dz \Theta[x(z)]$, as confirmed for specific examples below.

3. Phase transitions

While being sufficiently general to be applied to a large class of replicator models the above theoretical framework relies crucially on the assumptions made with respect to ergodicity, weak long-term memory, and the stability of the fixed point which the dynamics is assumed to approach asymptotically. A breakdown of this theory may thus be signalled by the failure of any of these assumptions, marking a dynamical phase transition at which the ergodic regime ceases to exist. In general one may imagine the following phenomena to occur:

- (i) The analytical ergodic theory resulting in Eqs. (20,21,22) might predict the integrated response χ to diverge in some subset of the parameter space of the model. Such a transition has been observed in replicator models with Hebbian interactions [27], and below this transition the system is found to be non-ergodic.
- (ii) In a similar way the theory might *analytically* predict singularities in either q or κ . No such types of transitions seem to have been observed so far in studies of RRM[‡].
- (iii) The set of equations (20,21,22) might fail to have solutions for certain values of the control parameters, so that no ergodic states are allowed in this region of the phase diagram. We will discuss cases of this type in section 4.
- (iv) Our ergodic theory is based on the assumption that all trajectories of the system will evolve into fixed points asymptotically. An onset of instability of these fixed points against small perturbations will thus signal the breakdown of our theory as they will no longer be local attractors of the dynamics. Such transitions have been observed in RRM with Gaussian and Hebbian couplings in [8, 9, 27].
- (v) Finally a breakdown of our requirement that long term memory be weak would indicate that the system remembers perturbations during the transient dynamics. Even if the system still evolves into a fixed point the latter might no longer be unique and the choice of the asymptotic stationary state might thus depend on initial conditions or perturbations at early stages of the temporal evolution. This type of transition has been related to the previous one (instability of the assumed fixed point) in [27], and we will demonstrate below that the conditions for both types of transitions are indeed fulfilled at the same points in parameter space whenever a replicator system with symmetric couplings is considered.

Transitions of the types (i)-(iii) are easily detected in numerical solutions of Eqs. (20,21,22). In the following we will therefore focus on (iv) and (v) and will derive explicit conditions for the onsets of instability and of memory at finite integrated response respectively.

[‡] Phases in which $\lim_{N \rightarrow \infty} q^{-1} = 0$ have been hinted at in [10] and will be discussed in more detail below. Note however that in these cases the equations describing the ergodic states do not analytically lead to singularities in q , but do not allow for any solutions at all in the phases where q is found to diverge in simulations; they are of the type (iii) in the above list of possible transitions.

3.1. Instability of the fixed point

In order to inspect the stability of the assumed fixed point we will follow [8] and take into account small fluctuations $\varepsilon y(t)$ and $\varepsilon v(t)$ of the effective species concentration and the single-particle noise about their respective fixed points x and η :

$$x(t) = x + \varepsilon y(t), \quad \eta(t) = \eta + \varepsilon v(t). \quad (23)$$

Note that in the following we will only consider the case $x > 0$, as it usually turns out that the onset of instability in replicator systems is determined by the fixed points different from zero while the zero fixed points remain stable against perturbations [8, 27].

From (23) we have

$$\langle x(t)x(t') \rangle_{\star} = q + \varepsilon^2 \langle y(t)y(t') \rangle_{\star}, \quad (24)$$

$$\langle \eta(t)\eta(t') \rangle_{\star} = \lambda + \varepsilon^2 \langle v(t)v(t') \rangle_{\star} \quad (25)$$

(fluctuations are taken to be uncorrelated with the fixed point values). The self-consistency condition on the covariance of the single-particle noise then implies

$$\langle v(t)v(t') \rangle_{\star} = \Lambda_1[\mathbf{C}, \mathbf{G}, \mathbf{D}](t, t'), \quad (26)$$

where Λ_1 is the first coefficient in the expansion

$$\Lambda[\mathbf{C} + \varepsilon^2 \mathbf{D}, \mathbf{G}](t, t') = \Lambda_0[\mathbf{C}, \mathbf{G}](t, t') + \varepsilon^2 \Lambda_1[\mathbf{C}, \mathbf{G}, \mathbf{D}](t, t') + \mathcal{O}(\varepsilon^4), \quad (27)$$

with $D(t, t') = \langle y(t)y(t') \rangle_{\star}$. Upon taking Fourier transforms of the time-translation invariant functions of $t - t'$ on both sides of Eq. (26) we write

$$\langle |\tilde{v}(\omega)|^2 \rangle = \tilde{\Lambda}_1(\omega). \quad (28)$$

Insertion of (23) into the effective process (8) (for $x > 0$) furthermore leads to

$$\frac{d}{dt}y(t) = -x \left[f'(x)y(t) - \int_{-\infty}^t dt' R(t-t')y(t') + v(t) + \zeta(t) \right], \quad (29)$$

to first order. In Fourier space one has

$$\tilde{y}(\omega) = -\frac{\tilde{v}(\omega) + \tilde{\zeta}(\omega)}{\frac{i\omega}{x} + f'(x) - \tilde{R}(\omega)}. \quad (30)$$

Focusing on $\omega = 0$ one obtains

$$\tilde{D}(\omega = 0) = \langle |\tilde{y}(\omega = 0)|^2 \rangle_{\star} = \phi \times \left[\tilde{\Lambda}_1(\omega = 0) + 1 \right] \left\langle |f'(x) - \rho|^{-2} \right\rangle_{+}, \quad (31)$$

where

$$\langle F[x(z)] \rangle_{+} = \frac{\int Dz \Theta[x(z)] F[x(z)]}{\int Dz \Theta[x(z)]}. \quad (32)$$

The factor ϕ in (31) takes into account that (30) was derived for non-zero fixed points $x > 0$ and that fluctuations about zero fixed points do not contribute to $\tilde{D}(0)$. Since $\tilde{\Lambda}_1(\omega)$ depends (linearly) on $\tilde{D}(\omega)$ (31) allows one to solve for $\langle |\tilde{y}(0)|^2 \rangle_{\star}$:

$$\langle |\tilde{y}(0)|^2 \rangle_{\star} = \left[\left(\phi \times \left\langle |f'(x) - \rho|^{-2} \right\rangle_{+} \right)^{-1} - \lambda_1 \right]^{-1}, \quad (33)$$

where we write $\tilde{\Lambda}_1(\omega = 0) = \lambda_1 \tilde{D}(\omega = 0)$. The coefficient λ_1 is determined by the form of the expansion (27). In the examples considered below one has $\lambda_1 = \partial\lambda/\partial q$. We conclude that $\tilde{D}(0) = \langle |\tilde{y}(0)|^2 \rangle_*$ diverges when the square bracket on the right-hand-side of (33) vanishes, suggesting an onset of instability. $\langle |\tilde{y}(0)|^2 \rangle_*$ is predicted to become negative whenever the right-hand-side of (33) becomes negative, indicating a further contradiction. The onset of instability occurs at the point defined by

$$\phi\lambda_1 \left\langle |f'(x) - \rho|^{-2} \right\rangle_+ = 1, \quad (34)$$

whereas the fixed points are stable whenever this expression is strictly smaller than one.

3.2. Memory onset

While in the previous section we have related the breakdown of our ergodic theory to a local instability of the fixed point reached by the dynamics, we will now inspect for an onset of long-term memory at finite integrated response. This type of transition has been observed previously for example in Minority Games with self-impact correction or diluted interactions [25, 26], and can also be interpreted in terms of a breakdown of time-translation invariance, see [2] for details. It is also found in replicator systems with Hebbian interactions [27]. In order to see how solutions with memory bifurcate from the time-translation invariant ergodic states we will proceed along the lines of [2] and make the following ansatz for the response function

$$G(t, t') = G_0(t - t') + \varepsilon \hat{G}(t, t'), \quad (35)$$

where $\varepsilon \hat{G}(t, t')$ is a small contribution which breaks time-translation invariance. The starting point of the dynamics can here no longer be sent to $-\infty$. For an interpretation of the physical meanings of \mathbf{G}_0 and $\hat{\mathbf{G}}$ see [27]. Following [2] $\hat{\mathbf{G}}$ is taken to depend only on the (earlier) time t' asymptotically, i.e. $\lim_{t \rightarrow \infty} \hat{G}(t, t') = \hat{G}(t')$.

Starting from (35) one expands the kernel of the retarded self-interaction in the effective process to linear order in \hat{G} , and finds

$$R(t, t') = R_0[\mathbf{C}, \mathbf{G}_0](t - t') + \varepsilon R_1[\mathbf{C}, \mathbf{G}_0, \hat{\mathbf{G}}](t, t') + \mathcal{O}(\varepsilon^2). \quad (36)$$

We will write $R_0(t - t') \equiv R[\mathbf{C}, \mathbf{G}_0](t - t')$ in the following. The effective process then becomes (to order ε)

$$\frac{d}{dt}x(t) = -x(t) \left[f(x(t)) - \int_0^t dt' R_0(t - t')x(t') - \varepsilon \int_0^t R_1(t, t')x(t') + \eta(t) - \kappa(t) \right] \quad (37)$$

so that fixed points are now found as $x = 0$ or as solutions of

$$f(x) - \rho x - \varepsilon \int_0^t dt' R_1(t, t')x(t') + \sqrt{\lambda}z - \kappa = 0, \quad (38)$$

where $\int_0^t dt' R_0(t - t')x(t') \equiv \rho x$ asymptotically for fixed point solutions $x(t) \rightarrow x$ as above. For any transient time t'' one then has

$$f'(x) \frac{\delta x}{\delta h(t'')} - \rho \frac{\delta x}{\delta h(t'')} - \varepsilon \int_0^t dt' R_1(t, t') \frac{\delta x(t')}{\delta h(t'')} = 0, \quad (39)$$

for $x > 0$, so that we can write

$$\varepsilon \widehat{G}(t'') = \left\langle \frac{\delta x}{\delta h(t'')} \right\rangle_* = \phi \varepsilon \int_0^t dt' R_1(t, t') \left\langle (f'(x) - \rho)^{-1} \frac{\delta x(t')}{\delta h(t'')} \right\rangle_+. \quad (40)$$

Again only trajectories leading to non-zero fixed points contribute, hence the factor ϕ . Note that the second term is also of order ε within our ansatz and that \mathbf{R}_1 depends linearly on $\widehat{\mathbf{G}}$. (40) can therefore be written as an eigenvalue problem $\widehat{G}(t) = \int dt M(t-t') \widehat{G}(t')$, with a suitable kernel \mathbf{M} [2]. Upon taking Fourier transforms and focusing on the zero frequency mode $\omega = 0$ one finds

$$\widehat{\chi} = \phi \langle |f'(x) - \rho|^{-2} \rangle_+ \rho_1 \widehat{\chi} = 0, \quad (41)$$

with the definition $\widehat{\chi} = \int dt \widehat{G}(t)$. We have here used (19) to write $\widetilde{M}(\omega = 0)$ in the form $\widetilde{M}(0) = \phi \langle |f'(x) + \rho|^{-2} \rangle_+ \rho_1$. ρ_1 is determined by the specific form of the term $\mathbf{R}_1[\mathbf{C}, \mathbf{G}_0, \widehat{\mathbf{G}}]$ in the expansion (36). In the examples considered below one has $\rho_1 \equiv \partial \rho / \partial \chi$. One sees that non-zero solutions for $\widehat{\chi}$ become possible at the point at which

$$\rho_1 \phi \langle |f'(x) - \rho|^{-2} \rangle_+ = 1 \quad (42)$$

We will refer to this as the memory onset (MO) condition.

One notices the close resemblance to the instability condition (34). Indeed for replicators with Hebbian couplings one has [27]§

$$\mathbf{R} = \alpha \mathbf{G}(\mathbf{I} + \mathbf{G})^{-1}, \quad \mathbf{\Lambda} = \alpha(\mathbf{I} + \mathbf{G})^{-1} \mathbf{C}(\mathbf{I} + \mathbf{G}^T)^{-1}, \quad (43)$$

where α is a control parameter of the model. Accordingly one finds

$$\lambda_1 = \rho_1 = \frac{\alpha}{(1 + \chi)^2} \quad (44)$$

and both conditions agree so that memory sets in at the same point at which the assumed fixed points become unstable. For interactions of the p -spin type known in the context of spin glasses (and which will be discussed in more detail for RRM in the next section) one has [23]

$$R(t, t') = \Gamma \frac{p(p-1)}{2} G(t, t') C(t, t')^{p-2}, \quad \Lambda(t, t') = \frac{p}{2} C(t, t)^{p-1}, \quad (45)$$

so that

$$\rho_1 = \Gamma \frac{p(p-1)}{2} q^{p-2}, \quad \lambda_1 = \frac{p(p-1)}{2} q^{p-2}. \quad (46)$$

within our fixed point ansatz $C(\tau) \equiv q$. The parameter $0 \leq \Gamma \leq 1$ here characterizes the symmetry of the couplings, and one finds that both the instability and MO conditions coincide for the case of fully symmetric couplings ($\Gamma = 1$). This appears to be the case more generally: in [28, 29] it is argued that for systems with dynamics based on a

§ Note the perturbation field h in [27] carries the opposite sign so that $\mathbf{I} - \mathbf{G}$ in [27] appears as $\mathbf{I} + \mathbf{G}$ in (43).

Langevin equation derived from a potential (i.e. for system with detailed balance) one usually has the relations of the type

$$R(t, t') = g'(C(t, t'))G(t, t'), \quad \Lambda(t, t') = g(C(t, t')) \quad (47)$$

with some (system-dependent) function $g(C)$ and $g' = dg/dC$ its derivative. Note that (47) implies $\lambda_1 = \rho_1 (= g'(q))$ in our notation. Although replicator dynamics are not of a gradient descent type, we expect the onsets of instability and memory to coincide whenever a system is considered in which the replicator equations can be derived from a Lyapunov function, and in particular for cases of fully symmetric couplings^{||}. Only in these cases does one find that the system evolves into fixed points also in the non-ergodic phases (see [9] and below). Fixed points are unique above the transition, but expected to be exponential in number below [7], hence the memory effects. For (partially) asymmetric couplings this is no longer the case, no fixed points are found below the transition; the MO-condition (derived based on the fixed point assumption) here fails to capture the breakdown of the ergodic theory.

4. Application to Gaussian random replicators

4.1. Model and stationary state

We will now apply the general theory developed in the previous sections to the case of replicator systems of second and higher-order interactions, with couplings drawn from a Gaussian distribution, in extension of the studies presented by other authors in [8] and [10].

Specifically, we will consider replicator equations of the form

$$\frac{d}{dt}x_i(t) = -x_i(t) \left[urx_i(t)^{r-1} + \sum_{(i_2, \dots, i_p) \in M_i^{(p)}} J_{i_2, i_3, \dots, i_p}^i x_{i_2}(t) x_{i_3}(t) \cdots x_{i_p}(t) - \kappa(t) \right], \quad (48)$$

with r and p fixed integers and where $M_i^{(p)} = \{(i_2, \dots, i_p) : 1 \leq i_2 < i_3 < \dots < i_p \leq N; i_2, \dots, i_p \neq i\}$. As above $\kappa(t)$ is chosen to ensure the constraint

$$\frac{1}{N} \sum_i x_i(t) = 1 \quad (49)$$

at any time t . The couplings $\{J\}$ are assumed to be drawn from a Gaussian distribution with zero mean and with variance and correlations as follows [22]

$$\overline{(J_{i_2, \dots, i_p}^i)^2} = \frac{p!}{2N^{p-1}}, \quad \overline{J_{i_2, \dots, i_p}^i J_{i_1, \dots, i_{k-1}, i_{k+1}, \dots, i_p}^{i_k}} = \Gamma \frac{p!}{2N^{p-1}}. \quad (50)$$

$\Gamma \in [0, 1]$ is a symmetry parameter of the distribution of couplings. For $\Gamma = 1$ their distribution is fully symmetric with respect to permutation of the indices, $\Gamma = 0$

^{||} Note to this end that replicator equations for which there exists a Lyapunov function H are of the form $\dot{x}_i = -x_i \left(\frac{\partial H}{\partial x_i} - \kappa \right)$ [7]. Thus $\frac{\dot{x}_i}{x_i} = -\frac{\partial H}{\partial x_i} + \kappa$ and the right-hand-side is identical to that of a Langevin equation (plus Lagrange parameter) so that the above relations (47) hold also in the effective process of such RMs.

corresponds to the case of fully uncorrelated couplings. Choosing $0 \leq \Gamma \leq 1$ allows one to interpolate smoothly between the two regimes.

The evaluation of the disorder-average in the generating functional can then be performed along the lines of [23] and one finds that the resulting effective process is of the form

$$\frac{dx(t)}{dt} = -x(t) \left[urx(t)^{r-1} - \Gamma \frac{p(p-1)}{2} \int_0^t dt' G(t, t') C(t, t')^{p-2} x(t') + \eta(t) - \kappa(t) \right], \quad (51)$$

so that the retarded interaction kernel reads

$$R(t, t') = \Gamma \frac{p(p-1)}{2} G(t, t') C(t, t')^{p-2}. \quad (52)$$

The covariance matrix of the effective single-particle noise comes out as

$$\Lambda(t, t') = \langle \eta(t) \eta(t') \rangle_{\star} = \frac{p}{2} C(t, t')^{p-1}. \quad (53)$$

Considering only fixed point solutions and making the above assumptions on ergodicity Eq. (18) can be written as

$$urx^{r-1} - \Gamma \frac{p(p-1)}{2} \chi q^{p-2} x + \left(\frac{p}{2} q^{p-1} \right)^{1/2} z - \kappa = 0 \quad (54)$$

in the present case.

We will now focus on the case $r = 2$ in which Eq. (54) becomes linear in x simplifying the further analysis considerably. Similar to [8, 27] we then have

$$x(z) = \frac{\kappa - \left(\frac{p}{2} q^{p-1} \right)^{1/2} z}{2u - \Gamma p(p-1) \chi q^{p-2} / 2} \Theta \left[\kappa - \left(\frac{p}{2} q^{p-1} \right)^{1/2} z \right]. \quad (55)$$

One also demonstrates that potential zero fixed points $x(z) = 0$ are unstable for positive arguments of the Θ -function, and that they are stable against perturbations otherwise. Eqs. (20,21,22) then take the explicit form

$$\left(\frac{p}{2} q^{p-1} \right)^{-1/2} \left(2u - \Gamma \frac{p(p-1)}{2} \chi q^{p-2} \right) = \int_{-\infty}^{\Delta} Dz (\Delta - z), \quad (56)$$

$$q \left(\frac{p}{2} q^{p-1} \right)^{-1} \left(2u - \Gamma \frac{p(p-1)}{2} \chi q^{p-2} \right)^2 = \int_{-\infty}^{\Delta} Dz (\Delta - z)^2, \quad (57)$$

$$\left(2u - \Gamma \frac{p(p-1)}{2} \chi q^{p-2} \right) \chi = \int_{-\infty}^{\Delta} Dz, \quad (58)$$

with $\Delta = \kappa / \left(\frac{p}{2} q^{p-1} \right)^{1/2}$. Here $Dz = \frac{dz}{\sqrt{2\pi}} e^{-z^2/2}$ is a standard Gaussian measure. We note that $\phi = \int_{-\infty}^{\Delta} Dz$ represents the probability of a given species i to survive in the long-term limit, i.e. to attain a fixed point value $x_i = \lim_{t \rightarrow \infty} x_i(t) > 0$. We will refer to ϕ as the fraction of surviving species in the following. For the case of symmetric couplings, $\Gamma = 1$, equations (56, 57, 58) are identical to those found in replica-symmetric studies of the statics of the model [10], and are readily solved numerically (in terms of κ , q and χ) as functions of the model parameters u and Γ (at fixed p).[¶] The conditions for the

[¶] Note here that the right-hand-sides of (56, 57, 58) can be written in closed form as functions of Δ after performing the Gaussian integrals over z . A solution of these equations can thus most efficiently be obtained by expressing $\{u, q, \chi\}$ as functions of Δ , and by subsequently varying Δ [14].

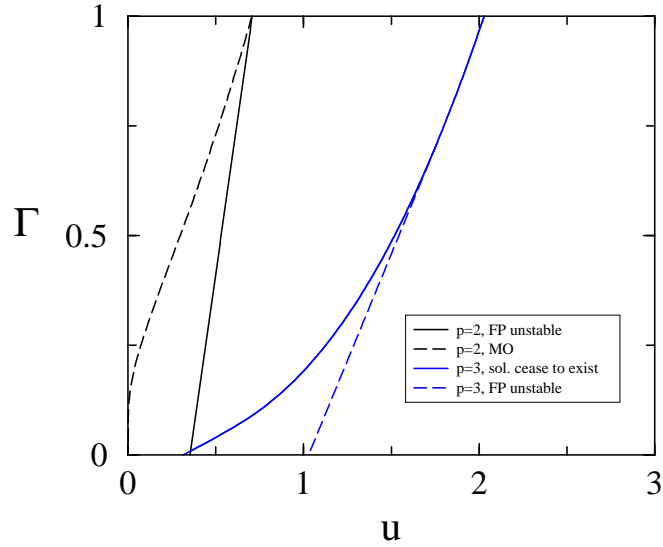


Figure 1. Phase diagram in the (u, Γ) plane for the model with Gaussian couplings and quadratic self-interaction ($r = 2$). The lines mark different transitions for the models with $p = 2$ and $p = 3$. Dashed line (left): onset of long-term memory for $p = 2$, see Eq. (42). Solid straight line: onset of the instability of the fixed points for $p = 2$, Eq. (59). Solid curve separates the region in which Eqs. (20)-(22) for $p = 3$ do admit a solution (high u) from the region in which no solutions are found. Dashed line to the right: fixed points become unstable for $p = 3$.

onsets of instability and memory (Eqs. (34) and (42)) take the form

$$\frac{p(p-1)q^{p-2}}{2\phi} \chi^2 = 1, \quad (59)$$

$$\Gamma \frac{p(p-1)q^{p-2}}{2\phi} \chi^2 = 1 \quad (60)$$

respectively. Our ergodic fixed-point solutions will turn out to be valid at values of u larger than some critical u_c . In particular we also note that (i) both conditions, (59) and (60), coincide for $\Gamma = 1$ as expected, (ii) the onset of the instability of the fixed point occurs before memory sets in for $\Gamma < 1$ (this follows from (59, 60) and the remark after (34)) and (iii) that the instability line is characterized by a condition on q , ϕ and χ , which can all be expressed as explicit functions of Δ using (56)-(58). Thus, the instability sets in at a fixed value of Δ , irrespective of the value of the model parameter Γ . Since Δ also fixes the combination $2u - \Gamma \frac{p(p-1)}{2} \chi q^{p-2}$ we conclude that (59) defines a line $u_c^{(p)}(\Gamma) = u_c^{(p)}(\Gamma = 0) + \Gamma(u_c^{(p)}(1) - u_c^{(p)}(0))$ in the (u, Γ) plane for any fixed value of p . After some algebra one finds that this simplifies to $u_c^{(p)}(\Gamma) = u_c^{(p)}(0)(1 + \Gamma)$ for replicator systems of the type studied here. The resulting phase diagrams for the models with $p = 2$ and $p = 3$ are depicted in Fig. 1, we will restrict the further discussion to these two specific cases. In both cases one finds that all assumptions regarding ergodicity and stability are fulfilled for high values of u , and that one of the assumptions breaks down at some value of u . The type of transition which occurs is different for the two models,

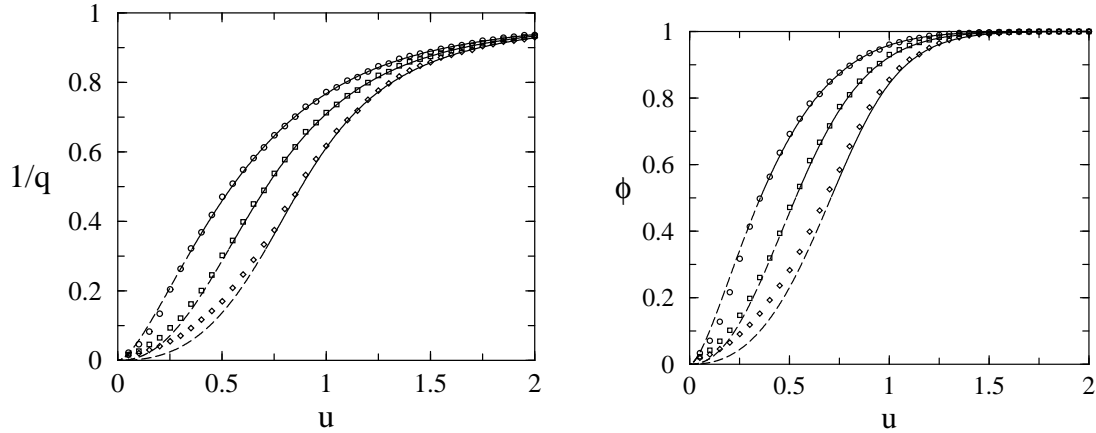


Figure 2. Inverse order parameter q and fraction of surviving species for the model with $p = r = 2$. Symbols are from simulations with circles corresponding to $\Gamma = 0$, squares to $\Gamma = 0.5$ and diamonds to $\Gamma = 1$. Simulations are for $N = 300$ species, run for 20000 steps and averaged over 50 samples of the disorder. Measurements are taken in the last quarter of the simulation. Initial conditions correspond to a flat distribution over the interval $[0, 2]$. ϕ is measured by applying a threshold $x_i > \vartheta$ to identify surviving species, a value of $\vartheta = 0.01$ is used here. The solid lines represent the analytical predictions in the ergodic phase, and have been continued as dashed lines below the transitions, where our theory is no longer valid.

and furthermore can depend on the value of Γ . We will discuss both models separately in the following.

4.2. The case $r = 2, p = 2$

We find that Eqs. (56,57,58) admit solutions for all u and Γ for $p = 2$ and we observe no singularities in any of the persistent order parameters. The predictions of the analytical theory for the order parameters in the ergodic phase are compared with numerical simulations⁺ in Fig. 2 and we find near perfect agreement at high values u . For $\Gamma \in \{0, 1/2\}$ theory and numerical experiment appear to agree well even at low values of u , only for $\Gamma = 1$ do we find systematic discrepancies below a critical value of u . The only possible violations of our assumptions of the ergodic stationary state are instabilities of the fixed points or an onset of long-term memory at finite susceptibility χ . The condition for onset of the instability of the fixed points (59) reduces to $u_c^{(p=2)}(\Gamma) = (1 + \Gamma)/(2\sqrt{2})$, as already derived in [8]. If one ignores this instability and continues the solutions of (56,57,58) to the right of the line $u = u_c^{(p=2)}(\Gamma)$ one finds that the memory onset condition Eq. (42) is fulfilled along the dashed line to the left in Fig. 1. As the fixed points are already unstable in this regime, this line has no direct physical meaning though, and is depicted only for illustration. We note that for $\Gamma = 1$ both the instability

⁺ A discretisation method similar to that of [9] is used. The typical (effective) time-step is of the order of $\Delta t \approx 0.01 - 0.1$.

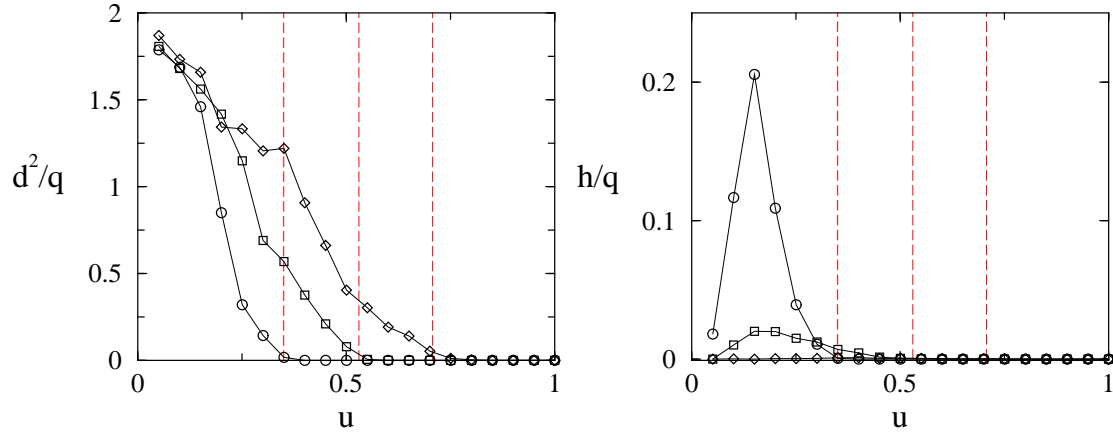


Figure 3. Relative distance d^2/q and roughness h/q versus u for the model with $p = r = 2$. Connected symbols are from simulations (circles: $\Gamma = 0$, squares: $\Gamma = 0.5$, diamonds: $\Gamma = 1$). d^2 obtained two runs at fixed disorder started from independent random initial conditions over $[0, 2]$. Parameters as in Fig. 2. Vertical dashed lines indicate the location of the phase transitions as predicted by the theory.

of the fixed point and the onset of memory occur at the same value of $u = 1/\sqrt{2}$. In the statics a de Almeida-Thouless instability is found at this point and replica symmetry is broken at smaller values of u [16].

To verify the onset of non-ergodicity further we have performed simulations in which two copies of the system with the same realization of the disorder are generated and in which the dynamics is started from two independent sets of random initial conditions drawn from a flat distribution over $x_i(0) \in [0, 2]$. The two resulting trajectories of the system are labelled by $\{x_i^a(t)\}$ and $\{x_i^b(t)\}$ respectively and we have measured the squared distance $d^2 = N^{-1} \sum_i (x_i^a(t) - x_i^b(t))^2$ in the stationary state. Results are depicted in Fig. 3. Note that we plot the ratio d^2/q , a value of $d^2/q = 2$ indicates uncorrelated stationary states. We find that d^2/q is essentially zero above $u_c(\Gamma)$, confirming the ergodicity and independence of the stationary state on initial conditions in this regime. Below u_c we find that $d^2/q > 0$, indicating the existence of multiple stationary states and the pronounced relevance of initial conditions.

We have secondly measured the relative ‘roughness’ h/q of the trajectories, where $h = N^{-1} \sum_i (\langle x_i(t)^2 \rangle_t - \langle x_i(t) \rangle_t^2)$ and $\langle \dots \rangle_t$ denotes a time-average in the stationary state. As shown in Fig. 3 all trajectories are flat ($h = 0$) irrespective of Γ above $u_c(\Gamma)$, verifying that the system indeed evolves into a fixed point in this regime. For symmetric couplings $\Gamma = 1$ this regime extends to lower values of u indicating that fixed points are also reached below the transition. For $\Gamma < 1$ we find non-zero values of h below the transition, so that we conclude that the system does not necessarily evolve into fixed points here*. This behaviour is also confirmed in Fig. 4 where we show typical

* The numerical data for h appears to show some dependence on system size, running time and time-window over which measurements are taken in the regime of volatile trajectories below $u_c(\Gamma < 1)$ (i.e.

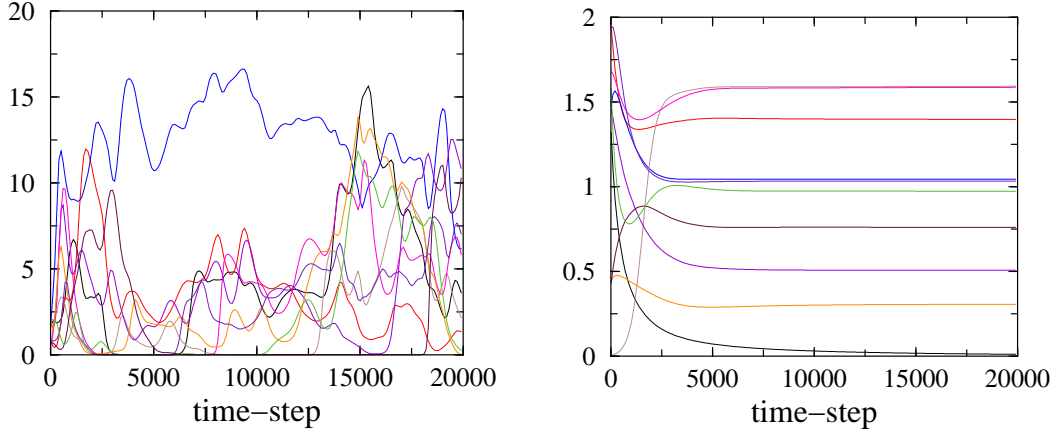


Figure 4. Trajectories $\{x_i(t)\}_t$ for 10 individual species in single runs of simulations of the model with $p = r = 2$ at fully asymmetric couplings, $\Gamma = 0$. Left: $u = 0.2$ below the transition, where fixed points are unstable, right $u = 1.0$ above the transition. Simulations are for $N = 500$ agents runs for 20000 time steps.

trajectories of the system at $\Gamma = 0$ (fully asymmetric couplings) below and above and the transition, see also [9] for a similar figure.

4.3. The case $r = 2$, $p = 3$

For $r = 2$ and $p = 3$ we find a distinctively different behaviour of the system. Eqs. (56, 57, 58) admit solutions only for $u > u^*(\Gamma)$, and below this value no ergodic fixed point solutions can be found. The obtained value $u^*(\Gamma = 1) \approx 2.028$ has already been reported in the context of a replica analysis of the model with symmetric couplings [10]. Note also that the limits $\lim_{u \downarrow u^*} q$, $\lim_{u \downarrow u^*} \chi$ and $\lim_{u \downarrow u^*} \kappa$ exist and take finite values. As indicated in Fig. 1 this type of transition is preceded by an onset of instability of the fixed points (determined by Eq. (59)) for values of $\Gamma < \Gamma_0 \approx 0.7$ in the sense that the instability sets in as u is lowered starting in the ergodic phase before solutions of the saddle point equations cease to exist. We note that the onset of instability again occurs along a line in the (u, Γ) plane, with $u_c^{(p=3)}(\Gamma) = u_c^{(p=3)}(0)(1 + \Gamma)$, where $u_c^{(p=3)}(0) \approx 1.028\#$.

Numerical results for the case $p = 3$ are presented in Fig. 5. Given the cubic interaction we limit ourselves to relatively small system sizes $N = 200$ and to moderate running times here. Results in the ergodic phases are however not affected significantly

when $h > 0$). The observations that fixed points are attained for all Γ above u_c and for all u for $\Gamma = 1$ are however not affected. More extensive simulations seem appropriate in order to check whether the apparently decreasing values of h as u approaches zero at $\Gamma < 1$ is genuine or a numerical artifact.

It turns out that Eqs. (56, 57, 58) have two branches of solutions above u^* , both solutions merge at u^* . For $\Gamma > \Gamma_0$ we find that the fixed points are stable along the physical branch and that the condition (59) for the onset of instability is fulfilled at $u_c^{(p=3)}(\Gamma) = u_c^{(p=3)}(0)(1 + \Gamma)$ only along the unphysical branch. Thus no instability is observed and a transition of the above type (iii) is the first one to occur when u is lowered from infinity. For $\Gamma < \Gamma_0$ the fixed point becomes unstable along the physical branch and the instability transitions precedes the failure of solutions to exist.

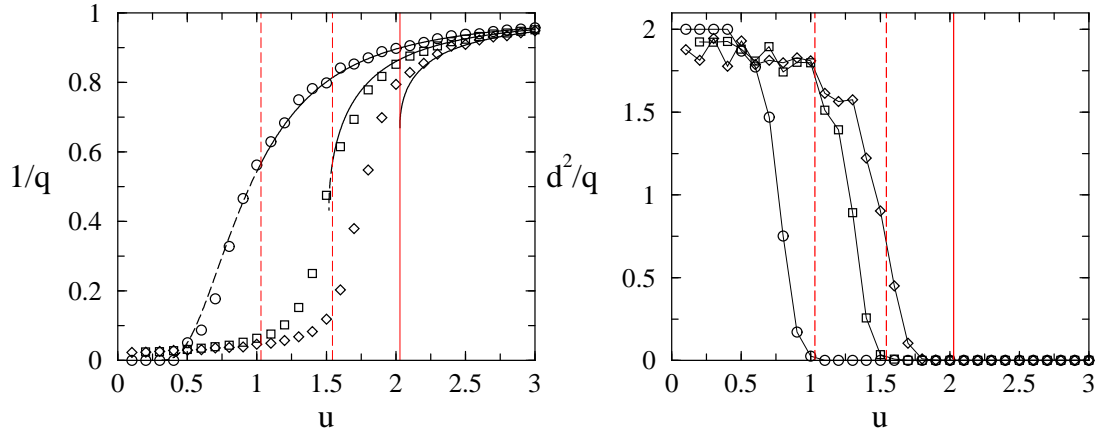


Figure 5. Reciprocal order parameter q and distance d^2 versus u for the model with $r = 2$ and $p = 3$. Symbols are from simulations (circles: $\Gamma = 0$, squares: $\Gamma = 0.5$, diamonds: $\Gamma = 1$). Solid lines for $1/q$ are the analytical predictions in the ergodic phase $u > u_c$. Vertical lines indicate the predicted locations of the transitions. Simulations were performed for $N = 200$ species, started from random initial conditions drawn with flat distribution from $x_i(0) \in [0, 2]$ and run for 3000 time-steps. Results are averages over 20 samples of the disorder.

by these constraints in computing time. We observe good agreement between the results for the order parameter q as obtained from theory and experiment, with only slight discrepancies close to the transitions due to finite-size effects. Note that results from simulations agree reasonably well with the theory for $\Gamma = 0$ also below $u = u_c$, where memory effects are already predicted to have set in, and where the ergodic does not apply strictly speaking. A similar (unexpected) agreement is also observed for $\Gamma = 0$ in the model with quadratic interactions $p = 2$, see Fig. 2. The right panel of Fig. 5 however confirms that non-ergodicity sets in at $u_c(\Gamma)$, indicated by non-zero distances between the stationary states obtained when starting the dynamics at fixed disorder from different random initial conditions as explained above^{††}. To summarise we have found a regime $u > \max(u_c(\Gamma), u^*(\Gamma))$ in which our ergodic theory applies and matches the simulations. For $\Gamma < \Gamma_0$ we then find an intermediate regime $u_* < u < u_c$ in which solutions of the saddle point equations exist, but in which the attained fixed points are unstable and the stationary state depends on initial conditions. No such intermediate regime appears to be found for $\Gamma > \Gamma_0$. Finally below u^* no solutions of the equations for the order parameters in the stationary ergodic state exist. The transition at u^* is not marked by any divergence in the analytic solutions for (q, χ, κ) as $u \downarrow u^*$.

To conclude this session we report some indications about the behaviour of the system below u^* based on numerical simulations. While the persistent order parameters

^{††}The slight discrepancy between the numerically observed onset of non-ergodicity and the value $u^* \approx 2.028$ at $\Gamma = 1$ is possibly due to the different nature of the transition. Below $u^*(\Gamma = 1)$ only a sub-extensive number of species appear to survive, as discussed below. However we cannot rule out finite-size or other numerical artifacts here.

converge to finite values in the limit of large N above u^* we observe strong finite size effects for $u < u^*$. The numerical data are consistent with power law behaviour $q \sim N^\gamma$ and $\phi \sim N^\delta$ with $\gamma > 0$ and $\delta < 0$ below u^* , see Fig. 6. This divergence of q with N seems to suggest that only a sub-extensive number of species $\phi N \sim N^{1+\delta}$ survives in this regime ($\delta < 0$) in the thermodynamic limit. Given the constraint $\lim_{N \rightarrow \infty} N^{-1} \sum_i x_i = 1$, we then conclude that these surviving species each must have concentrations scaling as $x_i \sim N^{-\delta}$, which in turn results in $q = N^{-1} \sum_i x_i^2 \sim N^{-\delta}$, i.e. we expect $\gamma = -\delta$. Within the accuracy of our simulations this is indeed what we observe, see Fig. 6. More precisely our simulations are consistent with $\gamma = -\delta = 1$ at low values of u , so that we expect only a *finite* number of species to survive in this regime ($\phi N \sim \mathcal{O}(N^0)$), even in the thermodynamic limit. This unusual effect is indeed confirmed upon plotting the number of species which are still alive as a function of time for different system sizes, see the right panel of Fig. 6. Note that closer inspection shows that the final number of surviving species in these simulations all fall into the range $10 \leq N\phi \leq 12$, even if the system size is varied by a factor of four from $N = 50$ to $N = 200$. A similar effect was observed in a replicator model with an explicit extinction threshold [17].

While our simulations confirm convincingly that $\gamma = -\delta = 0$ above u^* , and while they seem to suggest that $\gamma = -\delta = 1$ sufficiently far below the transition, the accuracy of our numerical experiments do not allow us to make any statement as to whether this onset of non-extensivity occurs continuously or discontinuously, i.e. whether the exponents drop instantly to zero when the transition at $u = u^*$ is crossed (from below) or whether one observes a cross-over.

5. Concluding remarks

In summary we have demonstrated how generating functionals can be used to study random replicator models. In the case of symmetric couplings this approach is able to reproduce the equations describing the ergodic stationary states obtained from static replica studies, but in addition the analysis of the dynamics also allows to address replicator systems with asymmetric interactions and to make accurate analytical predictions for the order parameters and phase diagrams.

Our analysis of Gaussian RRM indicates that the effect of asymmetry in the couplings is to increase the stationary value of the order parameter $1/q$ and with it the number of surviving species. This is the case for both models studies here, with interactions between $p = 2$ and $p = 3$ species respectively. Furthermore the range of the ergodic phases seem to be consistently larger the higher the degree of asymmetry in the couplings becomes. The symmetry or otherwise of the interactions also determines the behaviour of the system in the non-ergodic phases. Replicators with symmetric couplings evolve into fixed points in all regions of the phase diagram. In the symmetric case one expects a large number of such fixed points in the phase below u_c [7], and initial conditions determine which of these is reached, as indicated by the memory-onset. No

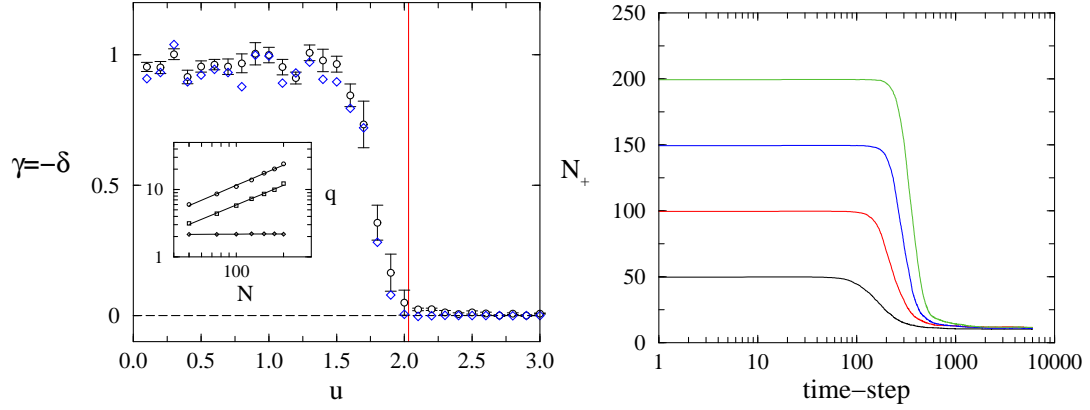


Figure 6. Left: Exponents γ (circles) and $-\delta$ (diamonds) (see text) as functions of u for the model with $r = 2$ and $p = 3$ ($\Gamma = 1$). Each data point is obtained by performing simulations at fixed u for $N = 50, 75, \dots, 200$, simulations are run for 6000 steps, averages over 10 samples of the disorder are taken, and subsequent fits to power laws $q \sim N^\gamma$ and $\phi \sim N^\delta$ are performed to obtain γ and δ . ϕ is measured as in Fig. 2. Vertical bars indicate the standard error of γ . Vertical solid line marks $u^*(\Gamma = 1)$. Inset: Log-log plots of q vs N for $u = 1.0$ (circles), $u = 1.5$ (squares) and $u = 2.5$ (diamonds) and the corresponding fits to power laws. (The data for q at $u = 2.5$ in the inset has been multiplied by a factor of two for convenience.) **Right:** Temporal evolution of the number N_+ of species with concentration $x_i(t) > \vartheta = 0.01$ for the same parameters, and at $u = 1$. Different curves are obtained from simulations of different system sizes $N = 50, 100, 150, 200$ from bottom to top.

such phase (and hence no MO transition) is found in models with asymmetric couplings. Instead, volatile trajectories are here observed below the transition, and individual species may come close to extinction $x_i(t) \ll 1$, but then recover to macroscopic values $x_i(t) \sim \mathcal{O}(1)$.

Models in which the self-interaction is of a lower order than the terms coupling distinct species appear to exhibit a phase in which the fraction of surviving species scales as $\phi \sim 1/N$, so that only a *finite* number of species survives in the long-run even in the thermodynamic limit. Possibly parallels with condensation effects in growth models of complex networks with quenched fitnesses of links and/or nodes can be drawn [30, 31].

While we have here concentrated on relatively simple systems of Gaussian couplings, the theory discussed in the first part of the paper might set the stage for further extension and application to more intricate models of replicators. These could include asymmetric dilution, multi-population models of game theory or dynamical models of chemical metabolic reactions, which progress in proportion to the concentration of reaction partners and in which stoichiometric coefficients might be modelled in terms of quenched random couplings.

Acknowledgements

This work was supported by the European Community's Human Potential Programme under contract HPRN-CT-2002-00319, STIPCO. The author would like to thank G Bianconi, A C C Coolen, M Marsili and D Sherrington for helpful discussions.

References

- [1] Challet D, Marsili M and Zhang Y-C 2005 *Minority Games* (Oxford University Press, Oxford UK)
- [2] Coolen A C C 2005 *The Mathematical Theory of Minority Games* (Oxford University Press, Oxford UK)
- [3] Johnson NF, Jefferies P and Hui PM 2003 *Financial market complexity* (Oxford University Press, Oxford UK)
- [4] Hofbauer J, Sigmund K 1988 *Dynamical Systems and the Theory of Evolution* (Cambridge University Press, Cambridge UK)
- [5] Peschel M, Mende W 1986 *The Prey-Predator Model* (Springer Verlag, Vienna)
- [6] Weibull J W 2002 *Evolutionary Game Theory* The MIT Press, Cambridge, Massachusetts
- [7] Diederich S, Opper M 1989 *Phys. Rev. A* **39** 4333
- [8] Opper M, Diederich S 1992 *Phys. Rev. Lett.* **69** 1616
- [9] Opper M, Diederich S 1999 *Comp. Phys. Comm.* **121-122** 141
- [10] de Oliveira V, Fontanari J 2000 *Phys. Rev. Lett.* **85** 4984
- [11] de Oliveira V and Fontanari J 2001 *Phys. Rev. E* **64** 051911
- [12] de Oliveira V and Fontanari J 2002 *Phys. Rev. Lett.* **89** 148101
- [13] de Oliveira V 2003 *Eur. Phys. J. B* **31** 259
- [14] Santos D, Fontanari J 2004 *Phys. Rev. E* **70** 061914
- [15] Tokita K 2004 *Phys. Rev. Lett.* **93** 178102
- [16] Biscari P, Parisi G 1995 *J. Phys. A: Math. Gen.* **28** 4697
- [17] Tokita K, Yasumoti A 1999 *Phys. Rev. E* **60** 842
- [18] Chawanya T, Tokita K 2002 *J. Phys. Soc. Japan* **71** 429
- [19] Rieger H 1989 *J. Phys. A: Math. Gen.* **22** 3447
- [20] De Dominicis C 1978 *Phys. Rev. B* **18** 4913
- [21] Simpson E H 1949 *Nature* **163** 688
- [22] Heerema M, Ritort F 1999 *Phys. Rev. E* **60** 3646
- [23] Crisanti A, Horner H, Sommers H-J 1993 *Z. Phys. B* **92** 257
- [24] Eissfeller H and Opper M 1992 *Phys. Rev. Lett.* **68** 2094
- [25] Heimel JAF, De Martino A 2001 *J. Phys. A: Math. Gen.* **34** L539
- [26] Galla T 2005 *J. Stat. Mech.* P01002
- [27] Galla T 2005 preprint [cond-mat/0507473](http://arxiv.org/abs/cond-mat/0507473)
- [28] Berthier L, Barrat J-L, Kurchan J 2000 *Phys. Rev. E* **61** 5464
- [29] Bouchaud J-P, Cugliandolo L, Kurchan J, Mezard M 1996 *Physica A* **226** 243
- [30] Bianconi G, Barabasi A-L 2001 *Phys. Rev. Lett.* **86** 5632
- [31] Bianconi G 2004 preprint [cond-mat/0412399](http://arxiv.org/abs/cond-mat/0412399)